23rd ABCM International Congress of Mechanical Engineering
December 6-11, 2015, Rio de Janeiro, RJ, Brazil

A NOVEL GHOST-CELL IMMERSED BOUNDARY METHOD FOR FLOW IN COMPLEX GEOMETRY

João Rodrigo Andrade
Aristeu da Silveira-Neto
João Marcelo Vedovoto
Federal University of Uberlândia - Campus Santa Mônica - bloco 5P - Avenida João Naves de Ávila - 2121 - bairro Santa Mônica - Uberlândia - MG - CEP 38400-902
jandrade@mec.ufu.br, aristeus@mecanica.ufu.br, jmvedovoto@mecanica.ufu.br

Abstract. *In the actual application of Computational Fluid Dynamics (CFD) a conforming grid is usually used to compute the flow around an arbitrarily moving or stationary body, especially for moving geometries that require a new mesh each time step, decreasing the efficiency of computing resources. In order to bypass this numerical problem, an innovative approach called Immersed Boundary Method (IBM) was developed to impose the boundary conditions of the solid body without the need of a grid reconstruction and requiring less computational efforts. In other words, an immersed boundary method is a methodology for dealing with a body which does not necessarily have to fit conform a Cartesian grid. The IBM requires two different meshes, a Eulerian Domain which is a grid that correspond to the flow field with no regard to the surface grid and a Lagrangian mesh that represents the solid body. The critical point of this approach consists on the interpolation function or numerical manipulation to link both meshes, modifying the equations in the vicinity of the boundary and exchanging information between then. Several different branches were developed based on the IBM, these treatments can be globally categorized into continuous forcing approach, discrete forcing approach, cut-cell methods, jump-singularities methods and approximated domain methods. This work presents a ghost-cell immersed boundary method for simulation flows in complex geometries, which enforces the boundary condition through a ghost cell method and interpolation functions. Dirichlet boundary conditions can be treated. The accuracy of the current method is validated using flows pas a circular cylinder and a sphere.*
Keywords: *Immersed-Boundary method, indirect iterative boundary condition imposition, body force interpolation function, ghost cell immersed boundary*

1. INTRODUCTION

The Immersed Boundary Method(IBM) was first proposed by Peskin (1977) to simulate blood flow in heart valves, a high complex problem that involves moving boundaries and complex geometries. The central idea of the Peskin method is the use of two independent meshes, an Eulerian mesh which is used to calculate the fluid flow equations and an independent Lagrangian mesh representing the immersed body. The communication between both meshes is made through a force source term added to the momentum equation. This procedure allows to model complex geometries immersed in a fluid flow, avoiding the use of complex meshes to fit the grid to the immersed body. As a geometric dependence does not exist between these two meshes, the immersed boundary method can easily handle moving boundary problems without regenerating grids in time. The main issue in the methods based on the concept of immersed boundary is how to compute the force term.

Since Peskin created this approach, many others researchers have been using the IBM successfully in various applications. Their applications cover a broad spectrum of fluid dynamics problems from flow through heart devices (Peskin 1972, Peskin 1977), to the interaction of body movement and fluid flow (Mittal, 2005), modeling anguilliform swimming (Tyson, 2008) and 3-D parachute simulation (Kim, 2009). Reviews of IB methods may be found in Mittal (2005) and Margnat (2009). Two classes of methods are discussed depending on how the source terms describing the presence of the boundary are imposed: directly in the continuous equations describing the flow (continuous forcing approach) or in the resulting system of linear equations (discrete forcing approach). Uhlmann (2005) presented a direct-forcing IB approach using the high-order regularized delta function suggested by Peskin (1972) in the velocity interpolation and the force distribution. The body force is distributed to adjacent Cartesian grids both inside and outside of the immersed boundary within a width of several grid spacings to give a smooth force transfer between the IB points and the Cartesian grids. According to Ji (2012) the correct calculation of the body force, which represents the fluid−solid boundary conditions, is a key issue for all type of IB approaches.

Several different immersed boundary methods can be found in the literature. They can be classified as either diffuse (continuous) methods or sharp (discrete) methods (Marella 2005, Martin 1996, Berthelsen 2008). The diffuse methods are considered to be considered no straightforward how the boundary conditions should be imposed at the immersed boundary. The boundary conditions are enforced through a smoothed forcing term added to the momentum equation (Berthelsen, 2008). One disadvantage with the diffuse methods is that the effect of the boundary is distributed over a band of several grid points which smear out discontinuities across the boundary. This smearing has an unfavorable effect on the accuracy of the numerical scheme (Berthelsen, 2008). Uhlmann (2005) distributed the body force both inside and outside of the immersed boundary over several grid spacing using the regularized delta functions suggested by Peskin (1977).

In present work, regarding the IBM, the multi-direct forcing method is adopted in this study. To impose a boundary condition on a solid object, we use a novel Ghost Cell Immersed Boundary Method. In this method, cells inside the solid body, called the ghost cells, are placed within a few grids from the interface in the solid region. The variables of fluid near the interface are extrapolated into the ghost cells to satisfy the boundary condition on the solid surface. We have used the ghost fluid method only for the calculation of velocity, the pressure boundary condition is computed by solving the pressure Poisson equation over all the computational domain, including the solid region like et al. (1997) and et al. (1999). A diffuse directional distribution forcing strategy which spreads the body force on ghost cells inside the immersed boundary is used on this model to prescribe the desired boundary conditions on immersed boundaries. The method also has some similarities to the ghost-cell method of Tseng (2003). There are no ad hoc constants introduced in the current procedure.

Numerical results of two distinct test cases which are simulated and compared to literature is presented, they are: a two-dimensional flow past a stationary circular cylinder at Reynolds number $Re = 40$ and $Re = 100$ and a three-dimensional flow past a stationary sphere at Reynolds number $Re = 100$. The turbulence modeling methodology used was the Large Eddy Simulation (LES) with the dynamic Smagorinsky algebraic sub-grid scale model (Germano et al., 1991) to calculate the turbulent viscosity. A fully implicit scheme is adopted for all cases calculated. The central difference scheme (CDS) is applied to express both the diffusive and advective contributions of the transport equations. Since the developed numerical code adopts a pressure-velocity coupling based on pressure variations, an appropriate algorithm for pressure-velocity coupling is needed.

2. METHODOLOGY

2.1 Mathematical Model for Fluid Domain

It was used the Navier-Stokes and continuity equations in the inertial reference frame, in order to solve the flow around an arbitrarily body. A rectangular domain was used for the present simulations and it was discretized with an Eulerian grid. The filtered Navier-Stokes equations for a viscous incompressible fluid can be written as Eq. 1.

$$\rho\left[\frac{\partial u_i}{\partial t}+\frac{\partial(u_i u_j)}{\partial x_j}\right]=-\frac{\partial p}{\partial x_i}+\frac{\partial}{\partial x_j}\left[(\nu+\nu_t)\left(\frac{\partial u_i}{\partial x_j}+\frac{\partial u_j}{\partial x_i}\right)\right]+f_i, \tag{1}$$

$$\frac{\partial u_i}{\partial x_i}=0, \tag{2}$$

Concerning turbulence modeling, Eq.1 is already shown as a filtered equation in a LES Framework, Eq. 2 is the continuity equation for incompressible flow. The Boussinesq hypothesis was used to model the subgrid Reynolds stress tensor.

2.2 Immersed Boundary Method

In this Section, some mathematical and computational information relevant to the used immersed boundary methods are presented. The present ghost-fluid based method consists of first identifying the image and the ghost points outside and within, respectively, the solid domain. From each lagrangian point in the boundary grid, a normal to the nearest boundary segment is built to locate these points that are not, necessary, co-located with the cartesian mesh. The value of the flow-field variables at each image point is then interpolated from the surrounding fluid points. The flowfield variables at the image point are subsequently reflected back to the corresponding ghost point to ensure the requisite boundary conditions. The image and ghost points are spaced ΔS from the immersed body, where ΔS is the average size of the edge of each lagrangian cell.

2.2.1 Interpolation and distribution strategies

To model the communication between Eulerian and Lagrangian meshes and set the boundary conditions, it is introduced two functions $I(\phi)$ and $D(\Phi)$ which represent the interpolation and distribution functions, respectively. For convenience the lower-case ϕ represents the variables on the fluid domain $\vec{x}$ (Cartesian grid, Eulerian domain), e.g. u, p, f, and the upper-case Φ indicates the variables on the IB points $\vec{X}_k$ (Lagrangian domain), such as U_k, F. The interpolation function projects these physical field from the image points to the ghost points carrying the immersed boundary information. On the other hand, the distribution function maps the physical field from the IB points back to the Cartesian grids.

The interpolation and distribution interaction function between the immersed boundary and the fluid are given by Eqs. 3 and 4, respectively.

$$\vec{\Phi}(\vec{X}_{IP},t) = I\left(\vec{\phi},\vec{X}_{IP},t\right) = \sum_{\vec{x}\in\Omega fluid} \vec{\phi}(\vec{x},t)\delta_h(\vec{x}-\vec{X}_{IP})\Delta V_i, \tag{3}$$

$$\vec{\phi}(\vec{x}_{GP},t) = D\left(\vec{\Phi},\vec{x}_{GP},t\right) = \sum_{\Omega_{solid}} \vec{\Phi}(\vec{X}_{GP},t)\delta_h(\vec{x}-\vec{X}_{GP})\Delta A_k \Delta S_k, \tag{4}$$

where, Ω_{fluid} represents the set of Cartesian grids outside the immersed boundary, Ω_{solid} represents the Lagrangian points over the immersed boundary, ΔV_i is the volume of control volume where the Lagrangian point k lies within, subscripts GP and IP stands for ghost point and image point, respectively, $\delta_h(\vec{x}-\vec{X}_k)$ is a weight-pondered function, in this work the function used is a hat function (Vedovoto, 2011), which gives a second order rate of convergence, with the advantage of requiring only one computational cell around the Lagrangian point k.

$$\delta_h(\vec{x}-\vec{X}_k) = \prod \frac{\varphi\left[(\vec{x}-\vec{X}_k)/\Delta x_i\right]}{\Delta x_i}, \tag{5}$$

where,

$$\varphi = \begin{cases} |1-r| & if\ r \leq 1 \\ 0 & if\ r > 1, \end{cases} \tag{6}$$

and r is the normalized distance between a Lagrangian point and the center of an Eulerian control volume where such Lagrangian point lies. The distribution/interpolation strategies is better illustrated in Fig. 1.

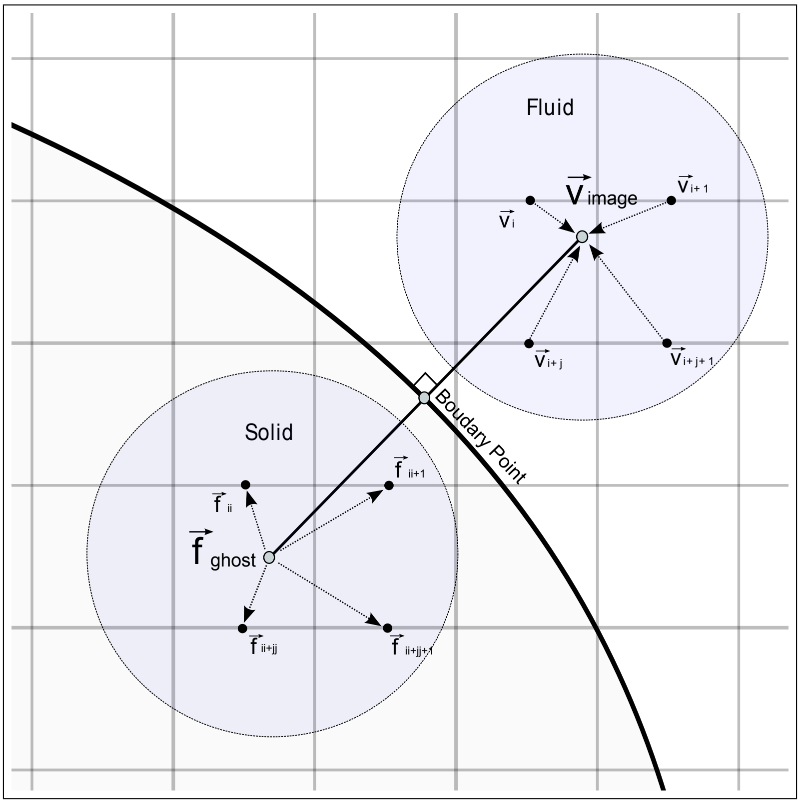

(a)

Figure 1. Schematic diagram for the interpolation strategy.

2.2.2 Computational Algorithm

First, an estimate of the velocity can be obtained by Eq. 7. Note that the Euler time discretization scheme is used here for the sake of simplicity. The subscript p stands for the inner loop of the IBM and start evaluated as $p = 1$.

$$\vec{u}^*_p(\vec{x}_k,t) = \vec{u}(\vec{x}_k,t)^n + \Delta t\left[r\vec{h}s\right]^n, \tag{7}$$

Next, the intermediate velocity at image points is obtained.

$$\vec{U}_p^*(\vec{X}_{IP},t) = I_d\left(\vec{u}_p^*, \vec{X}_{IP}, t\right). \tag{8}$$

Then, as the velocity at boundary point (d) is known, the force terms at ghost points are calculated.

$$\vec{U}_p^*(\vec{X}_{GP},t) = 2\vec{U}_d - \vec{U}_p(\vec{X}_{IP}^*,t). \tag{9}$$

$$\vec{F}_p(\vec{X}_{GP},t) = \frac{\vec{U}_p(\vec{X}_{GP},t) - \vec{U}_p^*(\vec{X}_{GP},t)}{\Delta t}. \tag{10}$$

The Lagrangian forces are distributed among the Eulerian ghost points.

$$\vec{f}_p(\vec{x}_{GP},t) = D_d\left(\vec{F}_p, \vec{x}, t\right). \tag{11}$$

Finally, the intermediate velocities are corrected.

$$\vec{u}_{p+1}^*(\vec{x}_{GP},t) = \vec{u}_p^*(\vec{x}_{GP},t) + \vec{f}_p \cdot \Delta t. \tag{12}$$

Check Eq. 13 for convergence, if the convergence is achieved then go to Eq. 14 otherwise go back to Eq. 7.

$$max\left|\vec{F}_{p+1}(\vec{x},t) - \vec{F}_p(\vec{x},t)\right| < \varepsilon, \tag{13}$$

$$\vec{u}(\vec{x}_{GP},t)^{n+1} = \vec{u}_{p+1}^*(\vec{x}_{GP},t). \tag{14}$$

3. RESULTS

In this section, the validation of the implementation are presented. Cases at various Reynolds numbers are compared between the original MDF, the ghost cell IBM and to the results reported by literature, cylinder case it is compared to Jungwoo Kim (2001) and Kravchenko and Moin (2000) and sphere case it is compared to Johnson (1999) and Kim (2002). In all following figures, unless the verified case, the flow direction is from left to right.

3.1 Laminar flow past 2D stationary circular cylinder

A laminar flow past a two-dimensional stationary circular cylinder, one of the benchmark problems, is calculated to verify the method developed in this work. This case has been investigated experimentally and numerically for many years. In this study, a domain with $W/D = 35$, $L/D = 50$ was adopted, where L is the domain horizontal length, W is the vertical length and D is the cylinder diameter. For our simulations at Reynolds number $Re = 40$ an $Re = 100$, a computational mesh of 714.100 volumes was used. The time step size was determined to make the maximum CFL number approximately equal to 0.25. A Dirichlet boundary condition $(u/u_\infty = 1; v = 0)$ is used at the inflow and farfield boundaries, the Dirichlet boundary is also used at cylinder surface $u = 0, v = 0$ and a Robin-type boundary condition is adopted at the outflow.

Figure 2 shows comparisons between the original MDF and the present method (ghost cell IBM) of the streamlines neighboring the cylinder for Reynolds number equal to 40 after the flow had reached a steady after symmetric state. The length of the recirculation zone, the location of the vortex centers and the angle of separation are given in Tab. 1, where they are compared with experimental and other numerical results. This indicates that the boundary condition is satisfied.

Figure 3 illustrates the iso-vorticity contours for $Re = 40 - 100$. Comparison is made among the ghost cell IBM, the

Table 1. Steady uniform flow past a circular cylinder for $Re = 40$: length L of recirculation zone, location (a, b) of vortex centre and separation angle θ (nomenclature given in Fig. 3).

	L/D	a/D	b/D	θ
Coutanceau (1977)	2.13	0.76	0.59	53.5
Linnick (2005)	2.28	0.72	0.60	53.6
Herfjord (1996)	2.25	0.71	0.60	51.2
Original MDF	2.25	0.75	0.60	54.0
Present study	2.27	0.76	0.62	52.0

original MDF and the literature results reported by Jungwoo Kim (2001). The good agreement is evident. The flow is

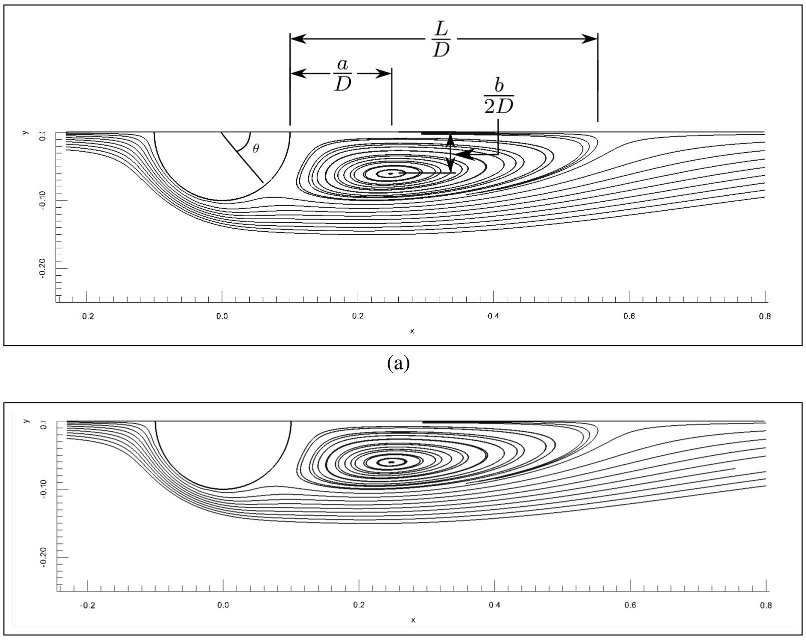

(a)

(b)

Figure 2. The streamlines for $Re = 40$ and nomenclature used in Tab. 1. (c) original MDF; (e) directional IBM.

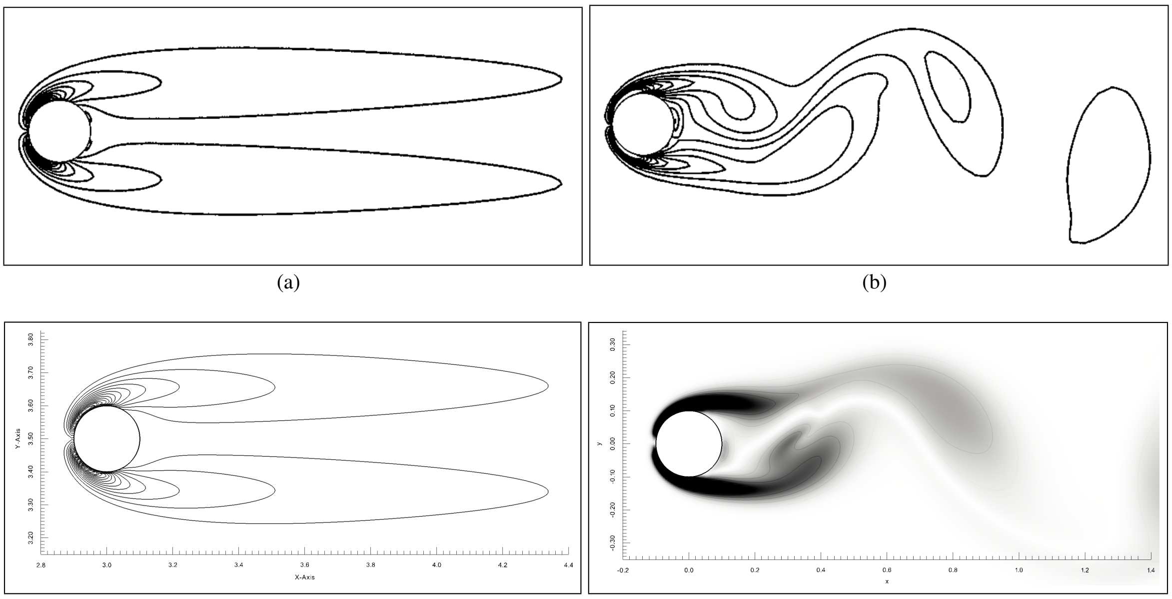

(a) (b)

(c) (d)

Figure 3. Iso-vorticity contours near a circular cylinder for $Re = 40$: (a) Jungwoo Kim (2001); (c) ghost cell IBM. For $Re = 100$: (b) Jungwoo Kim (2001); (d) ghost cell MDF. Instantaneous vorticity contours are drawn.

symmetric about the streamwise axis at $Re = 40$, whereas vortex shedding takes place at $Re = 100$, indicating that the vorticity field is well captured by the present immersed-boundary method.

Figure 4 shows a plot of the streamwise velocity u along the y axis for three lines with different distance from the cylinder center ($x/D = 15.55$,$x/D = 17.05$ and $x/D = 20.00$). The distribution indicates the decay of maximum velocity and increase of minimum velocity as the plot line increases the distances from the cylinder.

3.2 Flow past a sphere

A laminar flow past a three-dimensional stationary sphere, another well known benchmark problems, is calculated to verify the method developed in this work in a three dimensional case. A domain with dimensions $[25D, 10D, 10D]$ was adopted, in direction x, y and z, respectively, where D is the sphere diameter. For our simulations at Reynolds

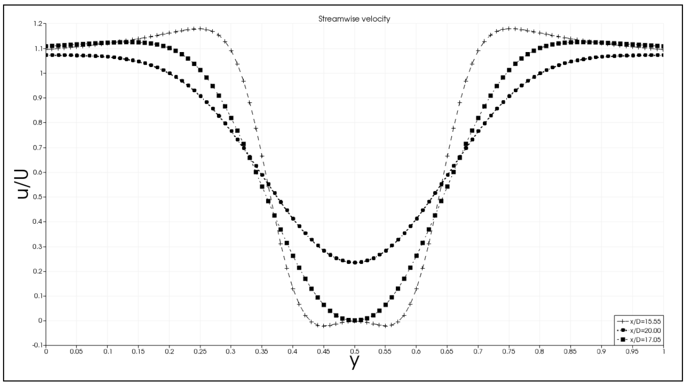

(a)

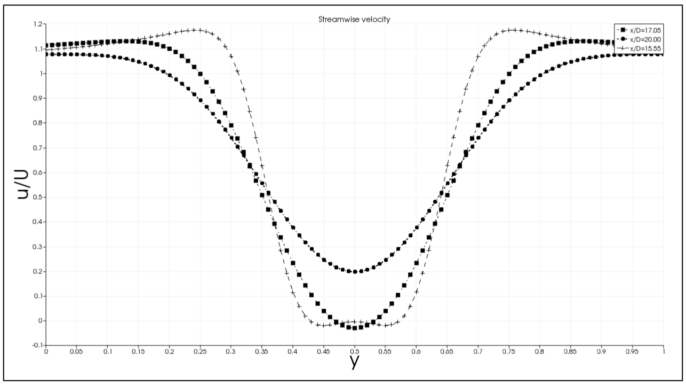

(b)

Figure 4. Streamwise velocity at y axis in different distances from the cylinder. (a) Ghost cell IBM and (b) multi-direct forcing approach.

number $Re = 100$, a computational mesh of $4.224.100$ volumes was used. The time step size was determined to make the maximum CFL number approximately equal to 0.25. On the surface of the sphere, the no-slip condition is applied, Dirichlet boundary condition $(u/u_\infty = 1; v = 0; w = 0)$ is used at the inflow and farfield boundaries, and a Robin-type boundary condition is adopted at the outflow.

Streamlines for this regime are shown in Fig. 5, which shows the (x, y)-planes for Reynolds number 100. The flow is seen to separate from the surface of the sphere at an angle θ and rejoin to form a closed separation bubble and a toroidal vortex, where the velocity is zero in the sphere's reference frame. The numerical results of Johnson (1999) provides data for comparison with the present results. Good agreement between the current results is shown.

Table 2. Steady uniform flow past a sphere for $Re = 100$.

	$x_c(m)$	$y_c(m)$	x_S(m)	$\theta_S(o)$
Johnson (1999)	0.72	0.26	1.23	126
Original MDF	0.77	0.25	1.29	125
Present study	0.78	0.29	1.34	128

4. RESULTS AND DISCUSSIONS

The results of the iterative IB method using the ghost cell strategy show good results, both original MDF and ghost IBM predicted very well the flow past the cylinder and the sphere.

5. ACKNOWLEDGEMENTS

The authors acknowledge CNPQ, CAPES, PROEX, PROPP, FAPEMIG and PETROBRAS for the financial support and the School of Mechanical Engineering of the Federal University of Uberlândia for the technical support.

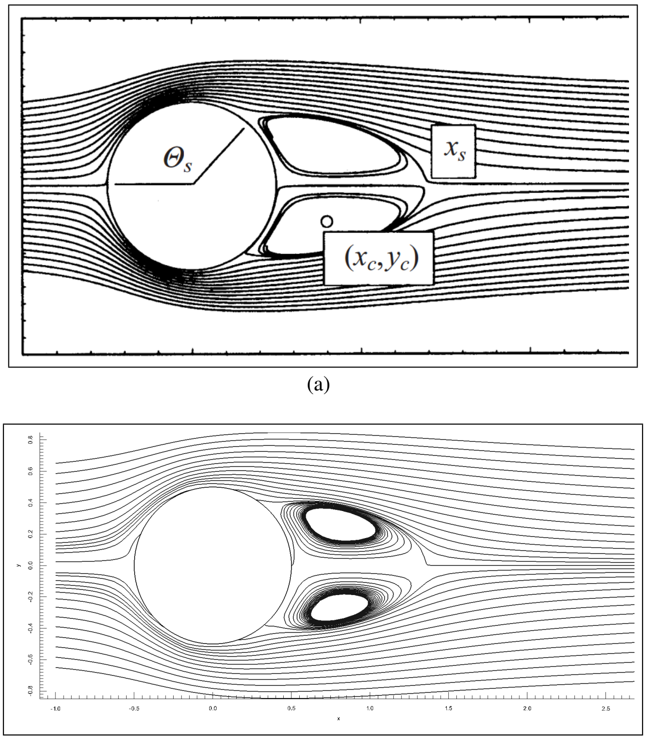

(a)

(b)

Figure 5. Computed axisymmetric streamlines past the sphere: (a)Johnson (1999) ; (b)ghost cell IBM.

6. RESPONSIBILITY NOTICE

The authors are the only responsible for the printed material included in this paper.

7. REFERENCES

Berthelsen, P. A.; Faltinsen, O.M., 2008. "A local directional ghost cell approach for incompressible viscous flow problems with irregular boundaries." *Journal of Computational Physics*, Vol. 227, 4354-4397.

Coutanceau, M. Bouard, R., 1977. "Experimental determination of the main features of the viscous flow in the wake of a circular cylinder in uniform translation part 1. steady flow." *J. Fluid Mech.*, Vol. 79:231-256.

et al., X., 1997. *Comput. Phys. Commun.*, Vol. 102, 147 1997.

et al., X., 1999. *J. Comput. Phys.*, Vol. 155, 348.

Herfjord, K., 1996. "A study of two-dimensional separated flow by a combination of the finite element method and navier-stokes equations." *Dr. Ing.-Thesis, Norwegian Institute of Technology, Department of Marine Hydrodynamics, Trondheim, Norway*.

Ji, C.; Munjiza, A.W.J., 2012. "A novel iterative direct-forcing immersed boundary method and its finite volume applications". *Journal of Computational Physics*, Vol. 231:1797-1821.

Johnson, T. A. Patel, V.C., 1999. "Flow past a sphere up to a reynolds number of 300." *Journal of Fluid Mechanics*, Vol. 378, 19-70.

Jungwoo Kim, ; Dongjoo Kim, a.H.C., 2001. "An immersed-boundary finite-volume method for simulations of flow in complex geometries." *Journal of Computational Physics*, Vol. 171,132-150.

Kim, D. Choi, H., 2002. "Laminar flow past a sphere rotating in the streamwise direction." *Journal of Fluid Mechanics*, Vol. 461, 365-386.

Kim, Y.P.C.S., 2009. "3-d parachute simulation by the immersed boundary method." *Computational Fluids*, Vol. 38:1080-90.

Kravchenko, A.G. and Moin, P., 2000. "Numerical studies of flow over a circular cylinder at red=3900." *Physics of Fluids*, Vol. 12, 403.

Linnick, M. N. Fasel, H., 2005. "A high-order immersed interface method for simulating unsteady compressible flows on irregular domains." *J. Comput. Phys.*, Vol. 204:157-192.

Marella, S.;Krishnan, S.L.H.H., 2005. "Sharp interface cartesian grid method i: an easily implemented technique for 3d moving boundary computations." *Journal of Computational Physics*, Vol. 210, 1-31.

Margnat, F.; MoriniÃÍre, V., 2009. “Behaviour of an immersed boundary method in unsteady flows over sharp-edged bodies.” *Computational Fluids*, Vol. 38:1065-79.

Martin, D.F.;Cartwright, K., 1996. “Solving poisson’s equation using adaptive mesh refinement.” *Technical Report UCB/ERI M96/66, U.C. Berkeley, California, USA*.

Mittal, R. Iaccarino, G., 2005. “Immersed boundary methods”. *Annual Reviews of Fluid Mechanics*, Vol. 37, 239-261.

Peskin, C., 1972. “Flow patterns around heart valves: A numerical method.” *Jounal of Computational Physics*, Vol. 10, 252-271.

Peskin, C., 1977. “Numerical analysis of blood flow in the heart.” *Jounal of Computational Physics*, Vol. 25:220-52.

Tseng, Y. Ferziger, J., 2003. “A ghost-cell immersed boundary method for flow in complex geometry.” *Journal of Computational Physics*, Vol. 192, 593-623.

Tyson, R. Jordan, C.E.H.J., 2008. “Modelling anguilliform swimming at intermediate reynolds number: a review and a novel extension of immersed boundary method applications.” *Computational Methods for Applied Mechanical Engineering*, Vol. 197:2105-18.

Uhlmann, M., 2005. “An immersed boundary method with direct forcing for the simulation of particulate flows.” *Journal of Computational Physics.*, Vol. New York, v. 209, p. 448-476.

Vedovoto, J.M., 2011. *Mathematical and numerical modeling of turbulent reactive flows using a hybrid LES / PDF methodology.* Ph.D. thesis.